individuals to at least some ideologically cross-cutting viewpoints (*4*). Of course, we do not pass judgment on the normative value of cross-cutting exposure. Although normative scholars often argue that exposure to a diverse "marketplace of ideas" is key to a healthy democracy (*25*), a number of studies have found that exposure to cross-cutting viewpoints is associated with lower levels of political participation (*22*, *26*, *27*). Regardless, our work suggests that the power to expose oneself to perspectives from the other side in social media lies first and foremost with individuals.

REFERENCES AND NOTES

1. K. Olmstead, A. Mitchell, T. Rosenstiel, *Navigating news online*. Pew Research Center (2011); available at www.journalism.org/analysis_report/navigating_news_online.
2. W. L. Bennett, S. Iyengar, *J. Commun.* **58**, 707–731 (2008).
3. E. Pariser, *The Filter Bubble: What the Internet Is Hiding from You* (Penguin Press, London, 2011).
4. S. Messing, S. J. Westwood, *Communic. Res.* **41**, 1042–1063 (2012).
5. E. Bakshy, I. Rosenn, C. Marlow, L. Adamic, *Proc. 21st Int. Conf. World Wide Web Pages* **1201.4145** (2012).
6. C. R. Sunstein, *Republic.com 2.0* (Princeton Univ. Press, Princeton, NJ, 2007).
7. N. Stroud, *Polit. Behav.* **30**, 341–366 (2008).
8. S. Kull, C. Ramsay, E. Lewis, *Polit. Sci. Q.* **118**, 569–598 (2003).
9. S. Flaxman, S. Goel, J. M. Rao, "Ideological segregation and the effects of social media on news consumption," SSRN Scholarly Paper ID 2363701, Social Science Research Network, Rochester, NY (2013).
10. T. Groeling, *Annu. Rev. Polit. Sci.* **16**, 129–151 (2013).
11. M. Gentzkow, J. M. Shapiro, *Q. J. Econ.* **126**, 1799–1839 (2011).
12. M. J. LaCour, "A balanced information diet, not echo chambers: Evidence from a direct measure of media exposure," SSRN Scholarly Paper ID 2303138, Social Science Research Network, Rochester, NY (2013).
13. E. Lawrence, J. Sides, H. Farrell, *Perspect. Polit.* **8**, 141 (2010).
14. D. O. Sears, J. L. Freedman, *Public Opin. Q.* **31**, 194 (1967).
15. N. A. Valentino, A. J. Banks, V. L. Hutchings, A. K. Davis, *Polit. Psychol.* **30**, 591–613 (2009).
16. L. A. Adamic, N. Glance, in *Proceedings of the 3rd International Workshop on Link Discovery* (ACM, New York, 2005), pp. 36–43.
17. S. Iyengar, K. S. Hahn, *J. Commun.* **59**, 19–39 (2009).
18. M. Duggan, A. Smith, "Social media update 2013," Pew Research Center (2013); available at www.pewinternet.org/2013/12/30/social-media-update-2013.
19. M. D. Conover, J. Ratkiewicz, M. Francisco, B. Gonçalves, A. Flammini, F. Menczer, Political polarization on Twitter. *Fifth International AAAI Conference on Weblogs and Social Media* (2011).
20. D. C. Mutz, J. J. Mondak, *J. Polit.* **68**, 140 (2006).
21. S. Goel, W. Mason, D. J. Watts, *J. Pers. Soc. Psychol.* **99**, 611–621 (2010).
22. D. C. Mutz, *Am. J. Polit. Sci.* **46**, 838–855 (2002).
23. B. Bishop, *The Big Sort: Why the Clustering of Like-Minded America Is Tearing Us Apart* (Houghton Mifflin Harcourt, New York, 2008).
24. D. C. Mutz, P. S. Martin, *Am. Polit. Sci. Rev.* **95**, 97 (2001).
25. T. Mendelberg, *Deliber. Particip.* **6**, 151–193 (2002).
26. R. Huckfeldt, J. M. Mendez, T. Osborn, *Polit. Psychol.* **25**, 65–95 (2004).
27. R. Bond, S. Messing, *Am. Polit. Sci. Rev.* **109**, 62–78 (2015).

ACKNOWLEDGMENTS

We thank J. Bailenson, D. Eckles, A. Franco, K. Garrett, J. Grimmer, S. Iyengar, B. Karrer, C. Nass, A. Peysakhovich, S. Taylor, R. Weiss, S. Westwood, J. M. White, and anonymous reviewers for their valuable feedback. The following code and data are archived in the Harvard Dataverse Network, http://dx.doi.org/10.7910/DVN/LDJ7MS: "Replication Data for: Exposure to Ideologically Diverse News and Opinion on Facebook"; R analysis code and aggregate data for deriving the main results (tables S5 and S6); Python code and dictionaries for training and testing the hard-soft news classifier; aggregate summary statistics of the distribution of ideological homophily in networks; and aggregate summary statistics of the distribution of ideological alignment for hard content shared by the top 500 most shared websites. The authors of this work are employed and funded by Facebook. Facebook did not place any restrictions on the design and publication of this observational study, beyond the requirement that this work was to be done in compliance with Facebook's Data Policy and research ethics review process (www.facebook.com/policy.php).

SUPPLEMENTARY MATERIALS

www.sciencemag.org/content/348/6239/1130/suppl/DC1
Materials and Methods
Supplementary Text
Figs. S1 to S10
Tables S1 to S6
References (*28*–*35*)

20 October 2014; accepted 27 April 2015
Published online 7 May 2015;
10.1126/science.aaa1160

ECOPHYSIOLOGY

Climate change tightens a metabolic constraint on marine habitats

Curtis Deutsch,[1]* Aaron Ferrel,[2]† Brad Seibel,[3] Hans-Otto Pörtner,[4] Raymond B. Huey[5]

Warming of the oceans and consequent loss of dissolved oxygen (O_2) will alter marine ecosystems, but a mechanistic framework to predict the impact of multiple stressors on viable habitat is lacking. Here, we integrate physiological, climatic, and biogeographic data to calibrate and then map a key metabolic index—the ratio of O_2 supply to resting metabolic O_2 demand—across geographic ranges of several marine ectotherms. These species differ in thermal and hypoxic tolerances, but their contemporary distributions are all bounded at the equatorward edge by a minimum metabolic index of ~2 to 5, indicative of a critical energetic requirement for organismal activity. The combined effects of warming and O_2 loss this century are projected to reduce the upper ocean's metabolic index by ~20% globally and by ~50% in northern high-latitude regions, forcing poleward and vertical contraction of metabolically viable habitats and species ranges.

Climate change is altering ecosystems by shifting distributions, phenologies, and interactions among species, but understanding how these changes are caused by climatic influences on physiology and fitness remains a challenge (*1*). In the ocean, increased metabolic rates due to rising temperatures will be accompanied by declines in dissolved O_2, potentially restricting organismal aerobic capacities (*2*–*4*). The physiology of hypoxic and thermal tolerance of marine species is well understood (*3*, *5*–*7*). Lacking, however, is a general mechanistic model that quantifies how O_2 and temperature jointly restrict large-scale biogeographic distributions now and in the future. Here, we combine laboratory and field data to demonstrate that temperature and O_2 together limit the contemporary ranges of marine ectotherms and to derive empirically based estimates of habitat loss in the warmer and less oxygenated oceans projected by this century's end.

For marine habitats to be metabolically viable, the environmental O_2 supply rate (S) must exceed an animal's resting metabolic demand (D). The rate of O_2 supply increases with ambient O_2 pressure (PO_2) and with respiratory efficacy (*8*). Thus, $S = \alpha_S B^{\delta} PO_2$, where respiratory efficacy is the product of α_s, a per-mass rate of gas transfer between water and animal and its scaling with body mass, B^{δ}. Resting metabolic demand also scales with B and with absolute temperature (T), according to $D = \alpha_D B^{\varepsilon} \exp(-E_o/k_B T)$, where α_D is a taxon-specific baseline metabolic rate, ε is its allometric scaling, E_o is its temperature dependence, and k_B is Boltzmann's constant (*9*).

We define a metabolic index, denoted Φ, as the ratio of O_2 supply to an organism's resting O_2 demand

$$\Phi = A_o B^n \frac{PO_2}{\exp(-E_o/k_B T)} \quad (1)$$

where $A_o = \alpha_s/\alpha_d$ is the ratio of rate coefficients for O_2 supply and metabolic rate, and n is the difference between the respective allometric scalings ($n = \delta - \varepsilon$). If Φ falls below a critical threshold value of 1, organisms must either suppress aerobic activity (*5*) or initiate anaerobic metabolism, conditions that are physiologically unsustainable. Conversely, values above 1 enable organismal metabolic rates to increase by a factor of Φ above resting levels, permitting critical activities such as feeding, defense, growth, and reproduction. Thus, for a given environment, Φ estimates the ratio of maximum sustainable metabolic rate to the minimum rate necessary for maintenance for a given species.

We analyzed data from published studies in which hypoxia tolerance was determined at

[1]School of Oceanography, University of Washington, Seattle, WA 98195, USA. [2]Department of Atmospheric and Oceanic Sciences, University of California, Los Angeles, CA 90095, USA. [3]Biological Sciences Department, University of Rhode Island, Kingston, RI 02881, USA. [4]Alfred Wegener Institute, D-27570 Bremerhaven, Germany. [5]Department of Biology, University of Washington, Seattle, WA 98195, USA.
*Corresponding author. E-mail: cdeutsch@uw.edu †Present address: Los Angeles Unified School District, Los Angeles, CA 90085, USA.

multiple temperatures (Fig. 1). Hypoxia tolerance was measured as the O_2 level below which the resting rate of metabolism cannot be maintained, anaerobic metabolic end products accumulate, or mortality increases. Such conditions correspond to the threshold value of $\Phi = 1$, allowing the parameters in Eq. 1 (n, E_o, and A_o) to be estimated (*10*). These parameters vary among species (table S1) due to differences in resting metabolic rates and oxygen uptake capacity (*11*–*14*). Within species, body mass weakly affected critical PO_2, PO_2^{crit} ($n = -0.3$ to 0) (fig. S1), suggesting that size-associated increases in O_2 uptake capacity (δ) largely compensate for increases in metabolic rate with size (ε) (*15*, *16*). Temperature on average accounted for 87% of the intraspecies variation in PO_2^{crit} (table S1), with slopes (E_o) for most of the species between 0.36 to 1.06 eV, similar to estimates for diverse physiological rates (*17*).

To evaluate whether the metabolic index limits the geographic range of species, we compared the spatial distributions of the index in the ocean with distributions of several marine species. Physiological and biogeographic data were available for four Atlantic species that live in diverse habitats (cod in open waters, rock crab in benthic zones, seabream in subtropics, eelpout in subpolar oceans) and differ widely in thermal and hypoxic tolerance (table S2). Using climatological temperature and O_2 data (*10*), we computed the seasonally varying three-dimensional distributions of the metabolic index. The global patterns of Φ are nearly identical among species because the patterns derive from environmental gradients of temperature and PO_2. Species differences in A_o scale the absolute values of Φ but not its spatial pattern, and variations in E_o only weakly alter the relative influence of temperature and O_2 gradients. The geographical distribution of Φ is also insensitive to whether O_2 uptake depends on the concentration, partial pressure, or diffusivity of O_2 in seawater (*10*, *18*) (fig. S2). Thus, when mapped relative to an arbitrary reference location, the spatial distribution and temporal variations in Φ are qualitatively independent of species.

For all studied species, the metabolic index in the upper ocean varies by more than 10-fold across latitude (Fig. 2A, values normalized to the tropical average), reflecting low subsurface PO_2 and high metabolic rates in tropical waters (low Φ) but generally high PO_2 and low metabolic rates in cooler, higher-latitude waters (high Φ). In contrast, vertical variation in Φ (Fig. 2B) is relatively small, because both temperature and O_2 decrease with depth and their individual effects on metabolic index are partly offsetting. In strong oxygen minimum zones (OMZs), however, O_2 declines more rapidly with depth than does metabolism, such that Φ decreases sharply with depth. Seasonal variability of Φ is generally small, except near OMZs, and in marginal seas and western boundary currents (fig. S3). Because the largest variations in Φ occur across latitude, we focus on whether latitudinal ranges of species are limited by the metabolic index.

From maps of the geographic distribution and metabolic index for the four focal species, we identified the occupied site where Φ was lowest: This was invariably at the southern (equatorward) range limit (Fig. 3). Across all species, seasons, and body masses, the minimum Φ varied only between 2 and 5 (table S3). Thus, marine environments appear viable only if they support metabolic rates at least 2 to 5 times resting rates. This critical metabolic index (Φ_{crit}) reflects not only the minimal physiological requirements for survival ($\Phi > 1$) but also additional energy required for key ecological activities ($\geq\Phi_{crit}$). Interestingly, sustained field metabolic rates of diverse terrestrial species are typically 1.5 to 5 times resting rates (*19*). This factorial increase is similar to values of Φ_{crit} of marine ectotherms, which suggests that it represents a fundamental metabolic requirement both on land and in the ocean but restricts the equatorial range limit only in the ocean.

Populations that migrate seasonally provide further support that the metabolic index restricts viable habitats. Western and eastern Atlantic cod share a common Φ_{crit} at their southern range border. Western cod migrate along the North

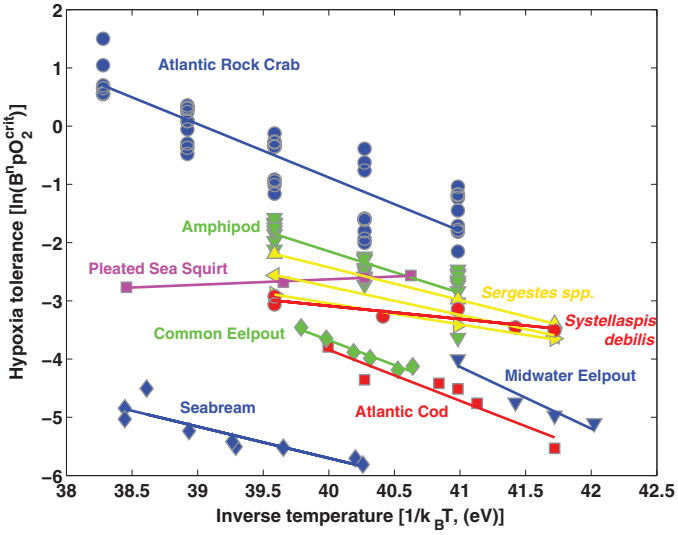

Fig. 1. Hypoxia tolerance versus inverse temperature. Laboratory data were compiled from published literature (see the supplementary materials) for 16 species in which hypoxic thresholds (PO_2^{crit}) were experimentally determined at three or more different temperatures. Of these species, 11 showed statistically significant relationships to temperature. Hypoxic thresholds are measured as the O_2 level below which the rate of metabolism cannot be maintained or an increase in mortality is observed. The parameters of the metabolic index are obtained from the slope (E_o) and intercept (A_o) of the linear regressions (table S1) (*10*).

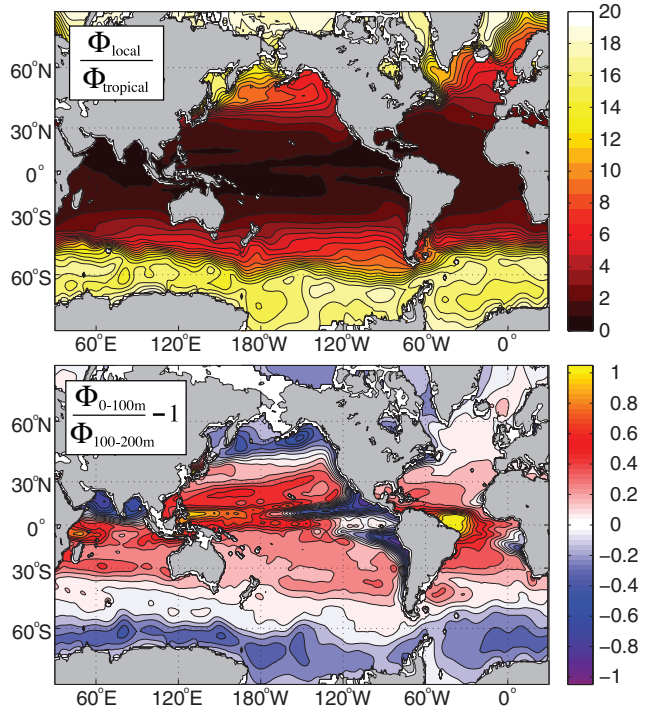

Fig. 2. Global relative distribution of metabolic index. The metabolic index is computed from climatological temperature and O_2 and normalized to depict large-scale patterns but not absolute values. Variation across latitude (**top**) is shown for the depth-averaged metabolic index of the upper ocean (0 to 200 m), divided by the mean value throughout the tropics (15°S to 15°N, 0 to 200 m). The metabolic index increases by >10-fold from the tropics to high latitudes due to the tendency for warm waters to have low O_2. Variation with depth (**bottom**) is computed as the relative difference between the average value in the upper 100 m and the average from 100 to 200 m. Negative values correspond to a decrease in Φ with depth. Vertical variations of Φ are reduced by the compensating decreases in both temperature and O_2 with depth but can be strongly negative in the presence of sharp OMZs. Both maps are computed with $E_o = 0.7$ eV, but the patterns depend only slightly on this parameter.

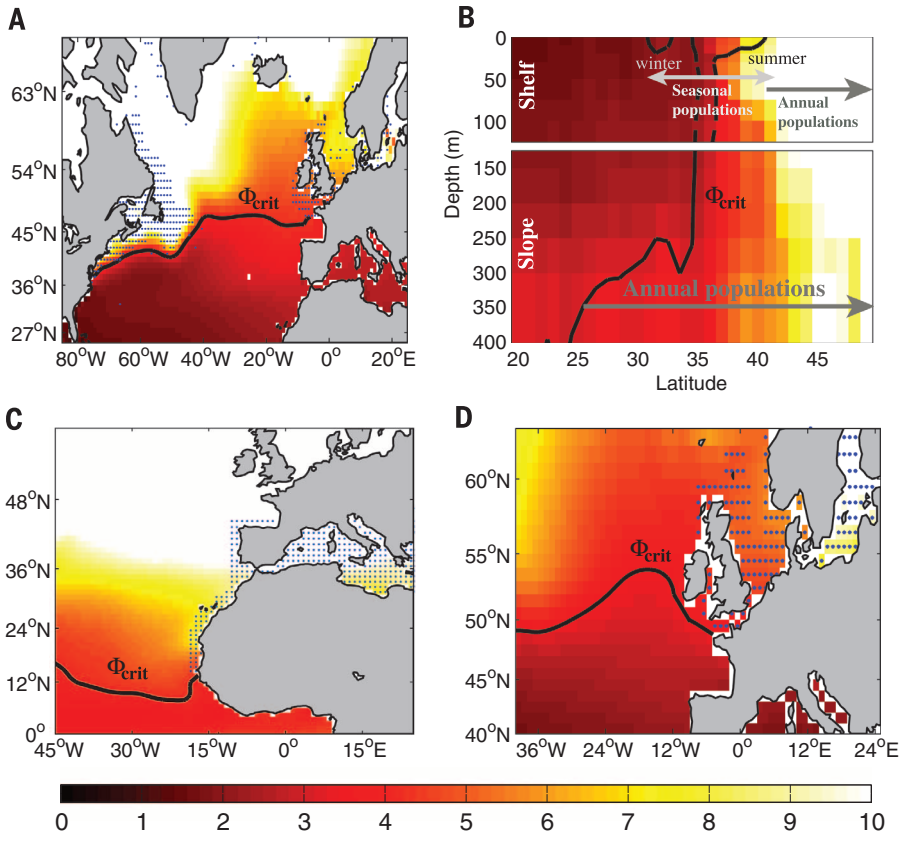

Fig. 3. Distribution of the metabolic index (Φ) in the Atlantic Ocean for all four species in Fig. 1 with documented marine population distributions. (**A**) Atlantic cod, (**B**) Atlantic rock crab, (**C**) sharpsnout seabream, and (**D**) common eelpout. For each species, Φ is averaged over its observed depth range (cod, 0 to 400 m; eelpout, 0 to 40 m; seabream, 0 to 60 m) except for rock crab, where values have been averaged over longitude in bottom grid cells along the North American margin. The minimum value found within the species distribution (Φ_{crit}) is contoured (black lines; values in table S3). For rock crabs, the contour of Φ includes both monthly maximum (winter) and minimum (summer) values above 100 m; below 100 m, it is cumulatively averaged downward along the slope at each latitude, to approximate the effect of seasonal movement of these crabs up and down the continental shelf. Occurrence data for each species are plotted (blue dots, interpolated to climate grid) for all species except crabs, whose latitudinal range of seasonal and year-round (annual) habitat in shelf and slope waters is indicated by gray arrows (see the supplementary materials).

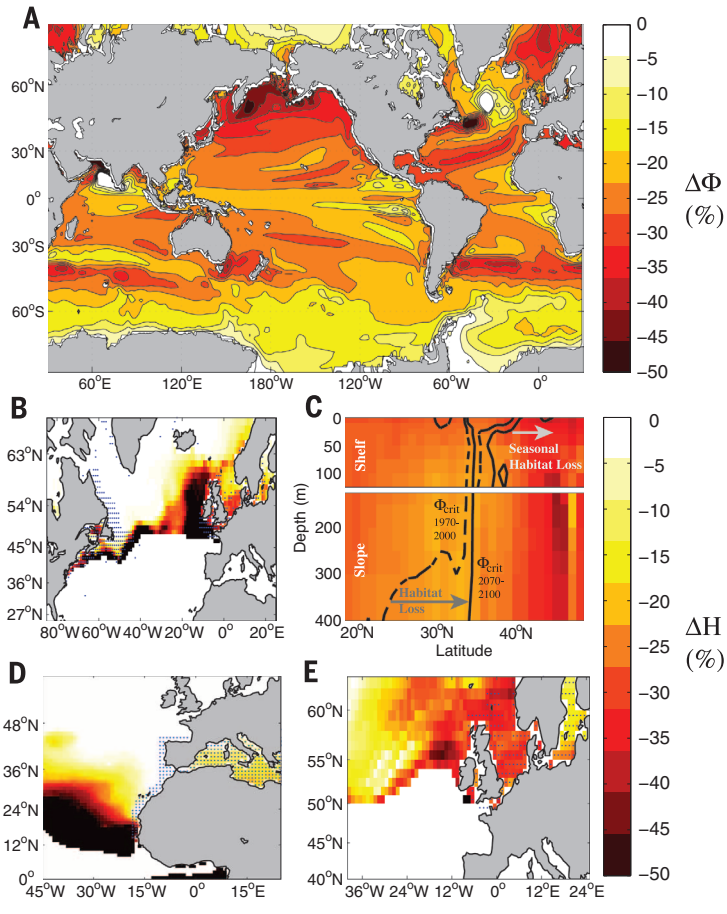

Fig. 4. Change in metabolic index and associated habitat compression from 1971–2000 to 2071–2100. (**A**) Global fractional change in Φ averaged over the upper 200 m, as projected by multiple Earth system model simulations under an 8.5 W/m^2 greenhouse gas emissions scenario (Representative Concentration Pathway 8.5), averaged across species. White areas indicate an increase in metabolic index, in all cases attributable to an increase in subsurface O_2. The individual contributions of changes in temperature and O_2 are shown in fig. S6. (**B** to **E**) Projected loss of metabolic habitat (denoted ΔH) for species with calibrated metabolic index values. Metabolic habitat is defined as any grid cell with $\Phi > \Phi_{crit}$ on a monthly basis. For cod (B), seabream (D), and eelpout (E), habitat changes are mapped as the percentage of change in annual mean thickness of the habitable water column between 1971–2000 and 2071–2100. For Atlantic rock crab (C), the background color map shows relative changes in Φ (%), and contours indicate the migration of Φ_{crit}. For all species, the relative change is an average over all months, so that the loss of habitat includes both vertical compression and a shortening of the habitable season.

American coast between 37°N in winter and 41°N in summer, paralleling seasonal shifts of Φ_{crit} (fig. S4A). Eastern cod migrate vertically, moving from cool temperatures in surface waters in winter to deeper waters in summer, in parallel with Φ_{crit} (fig. S4B). Seasonal migrations of benthic Atlantic rock crab also coincide with variations in Φ_{crit} in bottom waters (Fig. 3B). On the continental shelf, the latitudinal limits of seasonal crab populations in the mid-Atlantic Bight and of year-round populations north of 40°N are both delineated by a common Φ_{crit}. Deeper waters of the continental slope (100 to 400 m) have a metabolic index above Φ_{crit}, thus providing refugia for populations migrating from shallower shelf environments during summer (*10*).

Projected climate changes by this century's end (2071 to 2100) will affect the distribution of the metabolic index and thus of marine animals (Fig. 4). Climate models predict substantial warming and deoxygenation throughout most of the upper ocean (fig. S5 and table S4) (*10*). This implies global reductions in the metabolic index (Fig. 4A) throughout the upper water column (0 to 400 m), with a model-average decline of 21% (intermodel range 17 to 25%). Only ~1/3 of this reduction is attributable to O_2 loss, indicating that future marine hypoxia will be driven primarily by rising temperature, not by declining O_2 (*3*). The decline in Φ, and the relative contribution of temperature versus O_2, vary geographically (fig. S6). In mid-latitude Northern Hemisphere oceans—where fisheries are often highly productive—the metabolic index, and thus habitat suitability, should decline dramatically (~50%). The Pacific is prone to some of the largest reductions in Φ, driven by its larger projected fractional decrease in O_2 (figs. S5 and S6).

The focal species studied here illustrate how projected warming plus O_2 loss should shift metabolically viable habitats by century's end (Fig. 4, B to E). Habitable zones will often be vertically compressed and habitable seasons shortened throughout geographic ranges, but overall habitat losses are projected to be greatest near the equatorward edge of ranges, where Φ is low. For example, in the western subtropical Atlantic, where a wide swath of benthic habitat of rock crab is already close to Φ_{crit}, a 30% reduction in Φ would force a poleward retreat of slope populations from ~25°N to ~35°N. For other focal species, the average cumulative loss of habitat, measured as the reduction in currently occupied water volume with $\Phi > \Phi_{crit}$, ranges from 14 to 26% (table S5) (intermodel range 9 to 42%). These losses in aerobic habitat may be partially offset by habitat expansions where species ranges are now limited by cold tolerance.

Our results suggest that climate constraints on aerobic energy provision are the primary factors governing the equatorward range limit for diverse marine ectotherms. Thus, the metabolic index provides a simple but powerful metric linking physiology and biogeography with current and future environmental conditions. Even so, climate-forced ecosystem shifts will be complex, because changes in the metabolic index may be exacerbated by declines in net primary productivity (*20*), ocean acidification, and pollution (*1*), or ameliorated by acclimation and genetic adaptation (*21*). Biotic interactions will be altered because currently interacting species—if they have different metabolic sensitivities—will show noncoincident range contractions. Polar species may face increased competition caused by the invasion by lower-latitude species. Shallow-water predators may benefit from upwelling migrations of deeper water prey (*22*), and prey may benefit if their predators move away (*23*). Thus, climate shifts in the metabolic index may alter species ecologies even where metabolic indices exceed critical limits. Predictions of differential responses of ecologically interacting species to future shifts in metabolic indices will require more studies of temperature-dependent hypoxic tolerances, especially those of interacting and potentially interacting species.

REFERENCES AND NOTES

1. C. B. Field *et al.*, in *Climate Change 2014: Impacts, Adaptation, and Vulnerability. Part A: Global and Sectoral Aspects. Contribution of Working Group II to the Fifth Assessment Report of the Intergovernmental Panel on Climate Change*, C. B. Field *et al.*, Eds. (Cambridge University Press, Cambridge, UK and New York, NY, USA, 2014), pp. 35–94.
2. F. E. J. Fry, *Effect of the Environment on Animal Activity, University of Toronto Studies Biological Series No. 55* (Univ. of Toronto Press, Toronto, 1947).
3. H.-O. Pörtner, R. Knust, *Science* **315**, 95–97 (2007).
4. B. A. Seibel, *J. Exp. Biol.* **214**, 326–336 (2011).
5. P. W. Hochachka, *Trans. Am. Fish. Soc.* **119**, 622–628 (1990).
6. J. J. Childress, B. A. Seibel, *J. Exp. Biol.* **201**, 1223–1232 (1998).
7. H.-O. Pörtner, *J. Exp. Biol.* **213**, 881–893 (2010).
8. J. Piiper, P. Dejours, P. Haab, H. Rahn, *Respir. Physiol.* **13**, 292–304 (1971).
9. J. F. Gillooly, J. H. Brown, G. B. West, V. M. Savage, E. L. Charnov, *Science* **293**, 2248–2251 (2001).
10. See supplementary materials on *Science* Online.
11. B. A. Hills, G. M. Hughes, *Respir. Physiol.* **9**, 126–140 (1970).
12. B. A. Seibel, J. C. Drazen, *Philos. Trans. R. Soc. Lond. B Biol. Sci.* **362**, 2061–2078 (2007).
13. S. S. Killen, D. Atkinson, D. S. Glazier, *Ecol. Lett.* **13**, 184–193 (2010).
14. J. R. Friedman, N. E. Condon, J. C. Drazen, *Limnol. Oceanogr.* **57**, 1701–1710 (2012).
15. H. A. Woods, *Am. Zool.* **39**, 244 (1999).
16. G. E. Nilsson, S. Östlund-Nilsson, *Biol. Rev. Camb. Philos. Soc.* **83**, 173–189 (2008).
17. A. I. Dell, S. Pawar, V. M. Savage, *Proc. Natl. Acad. Sci. U.S.A.* **108**, 10591–10596 (2011).
18. W. C. E. P. Verberk, D. T. Bilton, P. Calosi, J. I. Spicer, *Ecology* **92**, 1565–1572 (2011).
19. J. R. Speakman, *Adv. Ecol. Res* **36**, 177 (2000).
20. L. Bopp *et al.*, *Biogeosciences* **10**, 6225–6245 (2013).
21. G. N. Somero, *J. Exp. Biol.* **213**, 912–920 (2010).
22. J. A. Koslow, R. Goericke, A. Lara-Lopez, W. Watson, *Mar. Ecol. Prog. Ser.* **436**, 207–218 (2011).
23. J. S. Stewart, J. C. Field, U. Markaida, W. F. Gilly, *Deep Sea Res. Part II Top. Stud. Oceanogr.* **95**, 197–208 (2013).

ACKNOWLEDGMENTS

Research was supported by the National Science Foundation (grants OCE-1419323, OCE-1458967, OCE-1459243, and ID 1038016), the Gordon and Betty Moore Foundation (grant GBMF3775 to C.D.), and the Polar regions and Coasts in a changing Earth System program (Alfred Wegener Institute). We thank the originators of the laboratory physiological data used here (available in the supplementary materials) and the individual climate modeling groups (table S4) and the World Climate Research Programme for producing and making available the CMIP5 model output. The technical support of H. Frenzel and the suggestions of K. Nagy, D. Jacobs, and two anonymous reviewers are gratefully acknowledged.

SUPPLEMENTARY MATERIALS

www.sciencemag.org/content/348/6239/1132/suppl/DC1
Materials and Methods
Supplementary Text
Figs. S1 to S6
Tables S1 to S5
References (*24*–*51*)

24 October 2014; accepted 5 May 2015
10.1126/science.aaa1605

CORAL REEFS

Limited scope for latitudinal extension of reef corals

Paul R. Muir,[1]* Carden C. Wallace,[1] Terence Done,[1,2] J. David Aguirre[3,4]

An analysis of present-day global depth distributions of reef-building corals and underlying environmental drivers contradicts a commonly held belief that ocean warming will promote tropical coral expansion into temperate latitudes. Using a global data set of a major group of reef corals, we found that corals were confined to shallower depths at higher latitudes (up to 0.6 meters of predicted shallowing per additional degree of latitude). Latitudinal attenuation of the most important driver of this phenomenon—the dose of photosynthetically available radiation over winter—would severely constrain latitudinal coral range extension in response to ocean warming. Latitudinal gradients in species richness for the group also suggest that higher winter irradiance at depth in low latitudes allowed a deep-water fauna that was not viable at higher latitudes.

The growth of phototrophic corals, those that rely on energy from endosymbiotic algae or "zooxanthellae," is determined by three primary latitude-correlated environmental factors (solar radiation, temperature, aragonite saturation) and by a number of factors not related to latitude (e.g., nature and depth of the substratum, wave climate, salinity, water quality, siltation regime) (*1*, *2*). Among the primary drivers of coral growth, only one—the amount of